NASA/TP-2002-211956

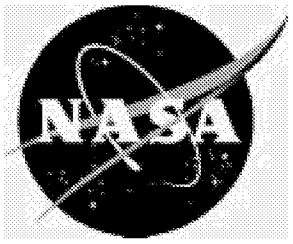

Geolocation Assessment Algorithm for CALIPSO Using Coastline Detection

J. Chris Currey
Langley Research Center, Hampton, Virginia

November 2002

The NASA STI Program Office ... in Profile

Since its founding, NASA has been dedicated to the advancement of aeronautics and space science. The NASA Scientific and Technical Information (STI) Program Office plays a key part in helping NASA maintain this important role.

The NASA STI Program Office is operated by Langley Research Center, the lead center for NASA's scientific and technical information. The NASA STI Program Office provides access to the NASA STI Database, the largest collection of aeronautical and space science STI in the world. The Program Office is also NASA's institutional mechanism for disseminating the results of its research and development activities. These results are published by NASA in the NASA STI Report Series, which includes the following report types:

- TECHNICAL PUBLICATION. Reports of completed research or a major significant phase of research that present the results of NASA programs and include extensive data or theoretical analysis. Includes compilations of significant scientific and technical data and information deemed to be of continuing reference value. NASA counterpart of peer-reviewed formal professional papers, but having less stringent limitations on manuscript length and extent of graphic presentations.

- TECHNICAL MEMORANDUM. Scientific and technical findings that are preliminary or of specialized interest, e.g., quick release reports, working papers, and bibliographies that contain minimal annotation. Does not contain extensive analysis.

- CONTRACTOR REPORT. Scientific and technical findings by NASA-sponsored contractors and grantees.

- CONFERENCE PUBLICATION. Collected papers from scientific and technical conferences, symposia, seminars, or other meetings sponsored or co-sponsored by NASA.

- SPECIAL PUBLICATION. Scientific, technical, or historical information from NASA programs, projects, and missions, often concerned with subjects having substantial public interest.

- TECHNICAL TRANSLATION. English-language translations of foreign scientific and technical material pertinent to NASA's mission.

Specialized services that complement the STI Program Office's diverse offerings include creating custom thesauri, building customized databases, organizing and publishing research results ... even providing videos.

For more information about the NASA STI Program Office, see the following:

- Access the NASA STI Program Home Page at ***http://www.sti.nasa.gov***

- E-mail your question via the Internet to help@sti.nasa.gov

- Fax your question to the NASA STI Help Desk at (301) 621-0134

- Phone the NASA STI Help Desk at (301) 621-0390

- Write to:
  NASA STI Help Desk
  NASA Center for AeroSpace Information
  7121 Standard Drive
  Hanover, MD 21076-1320

NASA/TP-2002-211956

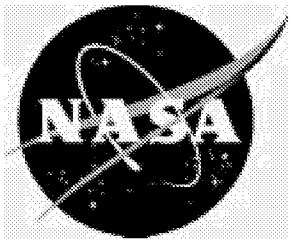

Geolocation Assessment Algorithm for CALIPSO Using Coastline Detection

J. Chris Currey
Langley Research Center, Hampton, Virginia

National Aeronautics and
Space Administration

Langley Research Center
Hampton, Virginia 23681-2199

November 2002

Acknowledgments

The author would like to thank Kam-Pui Lee, SAIC, for developing and modifying the powerful visualization tool, View_HDF, to support CALIPSO, and Mike Pitts, NASA, for leading the technical review of this paper.

Available from:

NASA Center for AeroSpace Information (CASI)
7121 Standard Drive
Hanover, MD 21076-1320
(301) 621-0390

National Technical Information Service (NTIS)
5285 Port Royal Road
Springfield, VA 22161-2171
(703) 605-6000

1. Summary

Cloud-Aerosol Lidar Infrared Pathfinder Satellite Observations (CALIPSO) is a joint satellite mission between NASA and the French space agency (CNES). The investigation will gather long-term, global cloud and aerosol optical and physical properties to improve climate models. The CALIPSO spacecraft is scheduled to launch in 2004 into a 98.2° inclination, 705 km circular orbit approximately 3 minutes behind the Aqua spacecraft. The payload consists of a two-wavelength polarization-sensitive lidar, and two passive imagers: the Wide Field Camera (WFC) operating in the visible (0.645 μm) and the Imaging Infrared Radiometer operating in the 8.7 - 12.0 μm spectral region. The imagers are nadir viewing and co-aligned with the lidar. Earth viewing measurements are geolocated to the Earth fixed coordinate system using satellite ephemeris, Earth rotation and geoid, and instrument pointing data. The coastline detection algorithm will assess the accuracy of the CALIPSO geolocation process by analyzing visible ocean land boundaries. Space-time coincident Moderate Resolution Imaging Spectrometer (MODIS) and WFC data will be processed with the coastline algorithm to verify co-registration. This paper quantifies the accuracy of the coastline geolocation assessment algorithm.

2. Introduction and Background

The coastline algorithm was first used for the Earth Radiation Budget Experiment (ERBE) scanner on the Earth Radiation Budget Satellite (ERBS) and the NOAA-9 spacecraft (Hoffman et al. 1987). The algorithm was refined for the Clouds and the Earth's Radiant Energy System (CERES) scanner and the Visible and Infrared Scanner (VIRS) on the Tropical Rainfall Measuring Mission (TRMM) (Currey et al., 1998). Implementation has been automated to collect and process clear scenes for the CERES instruments on the Terra and Aqua missions. The coastline algorithm is being used to verify boresight accuracy of the Atmospheric Infrared Sounder (AIRS) on Aqua (Gregorich and Aumann, 2002). Table 1 contains a listing of instruments and their respective field of view (FOV) sizes being analyzed with the coastline algorithm. A better understanding of the coastline algorithm uncertainties are required to determine suitability for assessing geolocation accuracy of higher resolution instrument data.

The CALIPSO geolocation process uses spacecraft ephemeris and attitude, Earth rotation and geoid, and instrument pointing vectors to calculate the latitude and longitude of each measurement location. The procedures used for geolocation are provided by the Earth Observing System (EOS) Science Data Production Toolkit. Estimated geolocation errors for CALIPSO measurements are approximately 1 km (3σ) at nadir. The coastline validation technique will detect biases post launch and verify these geolocation uncertainty estimates by analyzing visible coastal scenes from the Wide Field Camera. Processing space-time coincident MODIS and WFC scenes with the coastline algorithm will help verify CALIPSO and MODIS data co-registration for joint CALIPSO/Aqua retrievals.

The WFC imager is a pushbroom scanner with a single channel covering the 620 nm to 670 nm spectral range. The swath is 61 km wide centered on the lidar groundtrack. The central 5 km strip contains pixels at 125 m resolution; pixels outside the central strip are averaged onboard to produce 1 km pixels. The resultant image frame in Figure 1 consists of two low resolution swaths 28 km wide on each side of the central high resolution 5 km swath.

3. Algorithm Description

Clear coastal scenes with high surface reflectivity or emissivity gradients, i.e. deserts adjacent to ocean, make good targets for geolocation accuracy assessment. The diurnal reversal of the desert coastline signature allows processing of both day and night longwave scenes. For each coastal scene, an ensemble

of detected crossings is compared to a map database by minimizing the rms distance between the crossings and the map. A month of data is typically required to identify location systematic biases in the Earth fixed or instrument coordinate systems. ERBE coastline scenes were limited to four desert/ocean geographic sites: Baja, Northern Australia, Libya, and Oman. For TRMM additional targets along the southern coasts of Africa, Australia, and Mexico were processed using both shortwave and longwave data.

As a detector scans across a high contrast coastal scene a step response similar to Figure 2 is produced. The coastline signature is modeled using a cubic fit of four contiguous measurement samples

$$y_i = ax_i^3 + bx_i^2 + cx_i + d \tag{1}$$

where y_i is the measured radiance and x_i is pixel position (latitude or longitude). The coefficients are determined by solving the system of equations

$$\begin{bmatrix} a \\ b \\ c \\ d \end{bmatrix} = \begin{bmatrix} x_1^3 & x_1^2 & x_1 & 1 \\ x_2^3 & x_2^2 & x_2 & 1 \\ x_3^3 & x_3^2 & x_3 & 1 \\ x_4^3 & x_4^2 & x_4 & 1 \end{bmatrix}^{-1} \begin{bmatrix} y_1 \\ y_2 \\ y_3 \\ y_4 \end{bmatrix}. \tag{2}$$

The inflection point, $-b/3a$, is considered to be the location of the coastline if it falls between x_2 and x_3 and the change in radiance exceeds a predefined threshold.

The geolocation error for an individual scene is determined by fitting the ensemble of detected crossings to an accurate digitized map considered truth. The shift in geographical coordinates required to minimize the distance between the ensemble of coastline crossings and the map is defined as the geolocation error for an individual scene. Figure 3 depicts an ensemble of crossings simulated from a digitized map of Baja California with an error of –1.2° longitude and 0.2° latitude. The downhill simplex minimization algorithm (Press et al., 1988) iteratively shifts the ensemble of crossings until the rms crossing distance to the map is minimized. Scene geographic errors are transformed into spacecraft cross-track and along-track coordinates for correlation with possible error sources. Additional scenes are processed to identify systematic biases and trend performance of the instrument/satellite system.

CERES footprint locations were compared to the public domain CIA World Data Bank II map. Although no map accuracy numbers were available, a map error of less than 10% of the CERES FOV was assumed based on the coastline detection results of various TRMM VIRS scenes (Currey et al., 1998). Gregorich and Aumann (2002) detected significant biases between the World Data Bank II map and high accuracy USGS maps. Map accuracy determines how well the coastline algorithm can detect geolocation errors. More accurate and higher resolution maps are required for CALIPSO data analysis. The remainder of this paper presents results using two NOAA maps: the World Vector Shoreline (WVS) map and the Medium Resolution Digital Shoreline map.

The WVS map provides global coverage with a nominal scale of 1:250,000. The National Imagery and Mapping Agency (NIMA) requires that 90% of all identifiable WVS shoreline features be located within 500 meters circular error of their true geographic positions referenced to the World Geodetic System (WGS) 84 Earth model. The shoreline vertical datum is based on mean high water.

The Medium Resolution Digital Shoreline is a compilation of 270 NOAA nautical charts covering the contiguous United States of America from the most up-to-date charts available from 1988-1992. The resultant average mapping scale is approximately 1:70,000. The minimum adjacent vertex spacing is five meters ground distance.

Both map data are available from an online site, the "Coastline Extractor," hosted by the NOAA National Geophysical Data Center. Digitized map sections are easily extracted by specifying longitude and latitude (geodetic) ranges of interest. The Coastline Extractor tool is located at http://rimmer.ngdc.noaa.gov/coast/getcoast.html.

4. Simulation Results

The coastline algorithm is used to assess the accuracy of the geolocation process. Two calculations contribute to the uncertainty of the coastline algorithm: 1) finding imager coastline crossings, and 2) fitting the collection of coastline crossings to a map.

An understanding of the instrument point spread function (PSF) is required to accurately geolocate measurements (Smith, 1994). The PSF defines the effect of radiance at each point within the FOV on the measurement. Figure 4 shows the variation of the CERES scanner PSF theoretical model in the instrument along-scan and cross-scan coordinates. A field stop aperture restricts the sensor field of view to 1.3° in the along-scan direction and 2.6° in the cross-scan direction. The PSF peak value (diamond) is 1.36° and the PSF centroid (asterisk) is 1.51° behind the optical axis. The centroid is used to define the footprint location on the Earth surface for a given measurement time. Angular differences between the PSF peak and the PSF centroid must be accounted for in the geolocation accuracy assessment process.

The shape of the PSF determines the shape of the PSF step response; a symmetric PSF produces a symmetric PSF step response centered on the simulated coastline step input signature. Random sampling and a cubic model of the PSF step response determine the inflection point calculation uncertainty. The calculated inflection point is the assumed location of the coastline crossing. Figure 5 shows how the calculated inflection point (circles) varies for 100 different samplings and cubic fits of the PSF step response (thick line). Each iteration starts with four contiguous samples; a cubic polynomial is fit to the radiance signature, and the inflection point calculated. Sample pixels are shifted 0.01 pixels along-scan for the next iteration. Inflection points are compared to the true coastline location simulated by the step input location. Table 2 summarizes the accuracy of the inflection point approximation for two theoretical symmetric PSFs that vary in width. For both cases the mean inflection points are aligned with the step input. The Wide Field Camera PSF most closely resembles the first theoretical PSF in Table 2. For CALIPSO each coastline crossing should be detected within 0.53 pixels (3σ) of the true coastline.

The coastline detection process essentially samples the shape of the coastline. Fitting the collection of coastline crossings to a map determines the geolocation error for an individual scene. Table 3 presents map fitting results when various artificial geolocation shifts are added to crossings simulated from a reference map containing 1158 points of Baja California. Artificial shifts range from 1.2 degrees (~133 km) to 0.0001 degrees (~11 m). The number of crossings used in each ensemble varies from 4 to 1158. The factor in the first column indicates the ratio of the number of crossings to the number of map points used in the map fitting process. In all cases the number of crossings are fit to the Baja map containing 1158 points. This is an attempt to quantify the relationship between instrument resolution and map point spacing. A simplex is a geometrical figure consisting, in N dimensions, of N+1 points (or vertices) and the interconnecting line segments, polygonal faces, etc. (Press, 1988). In two dimensions the simplex is a triangle. For our application the simplex consists of three vertices containing the amount to shift each

ensemble of crossings in longitude and latitude coordinates. The starting simplex is the initial ensemble shift in three directions that bounds the maximum detectable geolocation error. The simplex vertex with the greatest map distance is adjusted for the next iteration. Processing continues until simplex ensemble map distances agree to within a specified fractional tolerance, typically 0.01. The number of function calls indicates how many times the ensemble map distance is calculated; one test case exceeded the limit of 1000 without convergence. The final longitude and latitude shift is opposite in direction to the artificial geolocation shift. The Xing-Map distance is the final shifted average crossing distance to the map. The Xing-Map distance indicates the "goodness" of the map fit and helps identify map sections with questionable accuracy. Xing-Map distances that greatly exceed the map resolution require further investigation. In all cases, except for the severe under-sampling of only 4 crossings, the ensemble is matched to the map and the correct shift determined. Table 3 shows that map point spacing and instrument resolution may vary by factors of 30 to 40, and still be used to accurately (< 1 %) detect geolocation shifts from 100 m to 100 km.

High resolution Advanced Spaceborne Thermal Emission and Reflection (ASTER) radiometer data are used to provide an empirical error analysis of the combined coastline detection and map fitting algorithms for CALIPSO. ASTER data are distributed by the U.S. Geological Survey's Earth Resources Observation Systems (EROS) Data Center Distributed Active Archive Center, located in Sioux Falls, South Dakota, and are available through the Earth Observing System Data Gateway. The Visible and Near Infrared (VNIR) Band 2 (0.63 – 0.69 μm) is used to simulate the CALIPSO WFC data. Data are specified in the Level 1 Data Products Specification, Version 1.2. Images contain 4100 pixels cross-track and 4200 pixels along-track at 15 m resolution. Longitude and latitude locations are saved as lattice points, 12 values along-track and 11 values cross-track. Coefficients for radiance conversion are provided for each of the 4100 pixels.

The first ASTER scene (Figure 6) processed with the coastline algorithm is of the entire island of Oahu, Hawaii, sampled June 3, 2000. The radiance threshold is set at 50 $Wm^{-2}sr^{-1}\mu m^{-1}$, with no cloud filtering or map distance threshold. Over 52,000 crossings are detected. The many false inland crossings on the southern coast of Oahu overestimate the bias at 2.35 km relative to the 1:250,000 World Vector Shoreline map (red circles). Coastline analysis using only the northern coast determines the bias to be 900 m, primarily in the spacecraft along-track direction. Other ASTER scenes along the coasts of Florida, California, and Baja have geolocation errors that vary from 200 - 5000 m with the majority of the error in the spacecraft along-track direction indicative of a timing problem. Both NOAA maps and ASTER data are referenced to the WGS 84 Earth surface model. Map latitudes are converted to geocentric coordinates to match ASTER data.

5. Algorithm Accuracy Estimation

The total coastline algorithm accuracy for CALIPSO applications is estimated from empirical data as follows:

- Start with a clear coastal non-industrialized high resolution scene (15 m)
- Run coastline detection and determine error between WVS map and high resolution data
- Add coastline detected offset to map to zero out error
- Simulate WFC data (125 m) from high resolution data using 2D PSF convolution
- Run coastline detection on 125 m data to determine error with shifted map
- Remaining error equals the uncertainty of the total coastline process

Figure 7 shows a clear coastal scene of Baja, California sampled along Sierra Vizcaino January 29, 2002 and centered at -114.0° longitude, and 27.0° latitude. Data are 15 m resolution from the VNIR Band 2 channel. Figure 8 shows 543 crossings (red symbols) detected from the coastline algorithm using a radiance threshold of 60 $Wm^{-2}sr^{-1}\mu m^{-1}$. No crossing map distance threshold is used; the majority of the crossings appear to track the land water boundary. The WVS map points (orange symbols) show the geolocation error for the scene. The ensemble map fitting process detects a mean bias of 4.99 km, with a standard deviation of 19 m (see Table 4). The final average shifted ensemble crossing distance to map is 95 m, indicative of a good fit for the scene. Figure 9 shows the same 15 m Baja scene with the WVS map shifted 4.99 km to match the apparent coastline indicated by the data. The bias between the data and map coastlines should now be eliminated. Figure 10 shows a small portion of the Baja peninsula near Punta San Hipolito where the maximum difference between the apparent coastline and the shifted WVS map section is approximately 200 m. The WVS map point spacing varies between approximately 35 and 75 m for this scene.

The original ASTER data are converted to 5 m resolution using bilinear interpolation, then convolved in two dimensions with the PSF discussed in Table 1, and finally subsampled to simulate the 125 m WFC data. Figure 11 shows the 71 coastline crossings detected using a radiance threshold of 50 $Wm^{-2}sr^{-1}\mu m^{-1}$. The average simplex shift and standard deviation are 48 m and 10 m respectively when minimizing to the shifted map. The final average crossing map distance is 85 m, indicative of a good fit for the scene. The remaining bias and standard deviation result in a total coastline algorithm accuracy of 78 m (3σ) for the simulated 125 m WFC data.

A theoretical estimate of the coastline algorithm uncertainty is as follows:

$$\sigma^2 = {\sigma_{CD}}^2 / N_{XINGS} + {\sigma_{MAP}}^2 / N_{MAP} \tag{3}$$

where σ_{CD} is the standard deviation of the coastline detection process (Table 2), σ_{MAP} is the standard deviation for an individual map point, N_{XINGS} are the number of coastline crossings detected for a scene, and N_{MAP} are the number of map points to which the ensemble distance is minimized. Using equation 3 the coastline algorithm theoretical estimate of uncertainty for this scene may be calculated. For the WVS map 90% of the map points are required to be within 500 m circular error of the true geographic position; therefore, the WVS map standard deviation, σ_{MAP}, equals 303 m. The 71 crossings detected should allow the scene geolocation error to be resolved within 108 m (3σ). This compares well with the empirical estimate of 78 m.

6. Algorithm Implementation

Figure 12 is along Sarasota Bay, Florida sampled October, 2001 from the ASTER instrument onboard Terra. VNIR Band 2 data are 15 m resolution. Sarasota/Bradenton International Airport is visible on the east side of the bay. This scene is not readily processed using the coastline algorithm due to the inhomogeneous surface reflectance and cloud contamination. Figure 13 shows map points from the 1:70,000 Medium Resolution Digital Shoreline manually shifted 0.005° north (~556 m) and overlaid along the apparent coastline. Figure 14 contains a second ASTER scene from Terra sampled October 15, 2001. The lower portion of the image contains data flagged bad by the ground processing system (black scans). The left portion of the image is of Clearwater Harbor; the lower right portion contains a causeway into West Tampa. Again the scene can not be processed due to cloud contamination and inhomogeneous surface reflectance. The map points are manually shifted 1.1 km north to visually match

the data coastline. Note the excellent alignment of the map and causeway. Clear scenes are required for accurate automated coastline results. Partially clear United States coastal scenes may be analyzed using the Medium Resolution Digital Shoreline map in this manual fashion.

During the first 90 days of the CALIPSO mission, initial checkout of the geolocation accuracy will use the 1:70,000 Medium Resolution Digital Shoreline map of the contiguous United States and an interactive visualization tool, View_HDF (Lee 2001), modified to support geolocation assessment. Partially clear coastal scenes may be analyzed by interactively shifting the high resolution map overlay to match the image data. Assuming no systematic biases in the Medium Resolution Digital Shoreline map, an assessment of the WFC geolocation accuracy may be quickly determined.

Figure 15 shows the result of processing the same Baja scene with the interactive visualization tool and the 1:250,000 World Vector Shoreline map. The red circles show the original location of the map points; the orange circles show the final map locations after interactively shifting the map 0.011° longitude and 0.044° latitude, or 5.034 km. The geolocation error detected using the automated coastline algorithm is –0.0105° longitude and –0.0436° latitude, or 4.993 km. The difference between the automated and manual processes is 41 m. The coastline detection algorithm will use the World Vector Shoreline map for automated processing of global clear desert coastal scenes.

7. Concluding Remarks

The CALIPSO coastline detection algorithm can assess the 125 m resolution Wide Field Camera geolocation accuracy to within 100 m by processing clear coastal desert scenes and fitting detected crossings to the 1:250,000 World Vector Shoreline map. The coastline algorithm may be fully automated or used in conjunction with an interactive visualization tool. Automation reduces the amount of labor but introduces complexity in scene selection and algorithm design. Scene errors may be introduced due to false coastline detections resulting from inhomogeneous surface reflectance and cloud contamination. Cloud edge detections may be eliminated with cloud masking with additional infrared data; for CALIPSO this requires the registration of the Infrared Imaging Radiometer data to the WFC grid.

8. References

Currey, J. C., G. L. Smith, and R. Neely, 1998: Evaluation of Clouds and the Earth's Radiant Energy System (CERES) scanner pointing accuracy using a coastline detection system, *Proc. SPIE*, Vol. 3439, July, 367-376.

Gregorich, D., and H. Aumann, 2002: Verification of AIRS boresight accuracy using coastline detection, submitted May 2002 to *Trans. On Geoscience and Remote Sensing.*

Hoffmann, L., W. Weaver, and J. Kibler, 1987: Calculation and accuracy of ERBE scanner measurement locations, NASA TP 2670, Sept., 13 pp.

Lee, K., 2001: View_HDF User's Guide, Version 3, September, 107 pp.
http://eosweb.larc.nasa.gov/HPDOCS/view_hdf.html

Press, W., B. Flannery, S. Teukolsky, and W. Vetterling, 1988: *Numerical Recipes in C*, Cambridge University Press, Cambridge, 713 pp.

Smith, L., 1994: Effects of time response on the point spread function of a scanning radiometer, *Applied Optics*, Oct., 7031-7037.

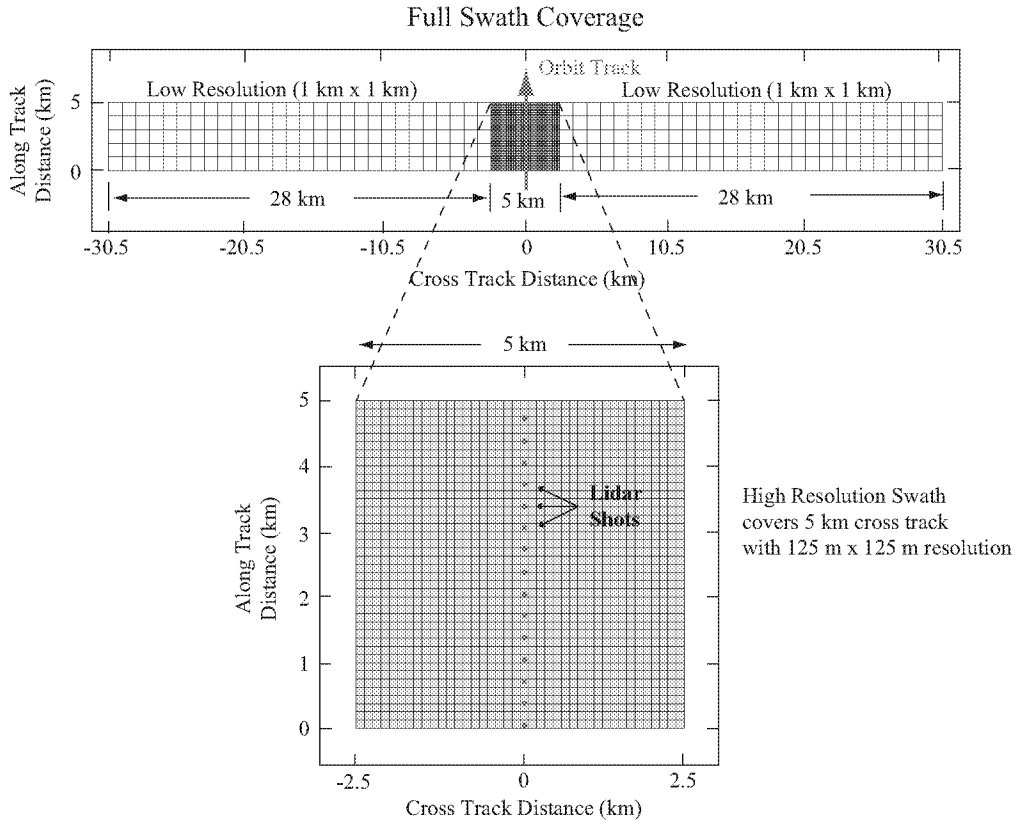

Figure 1. CALIPSO WFC frames accumulated along-track to build images.

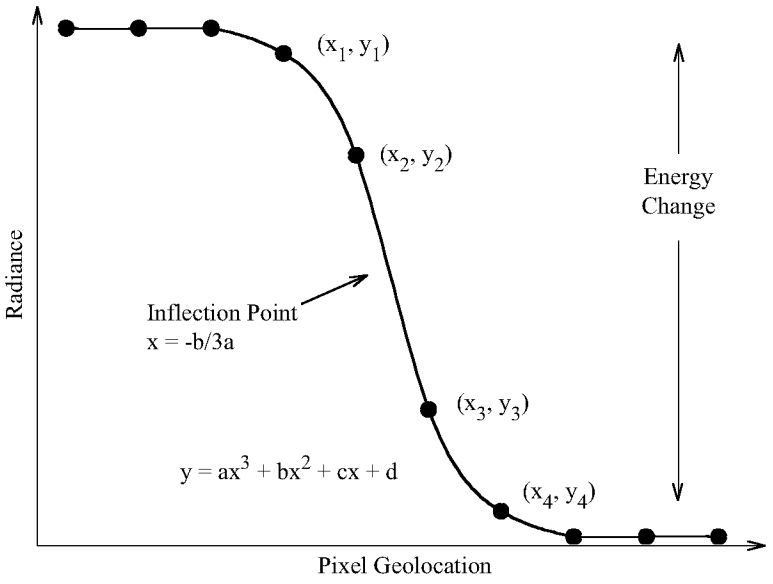

Figure 2. Determination of coastline crossing location.

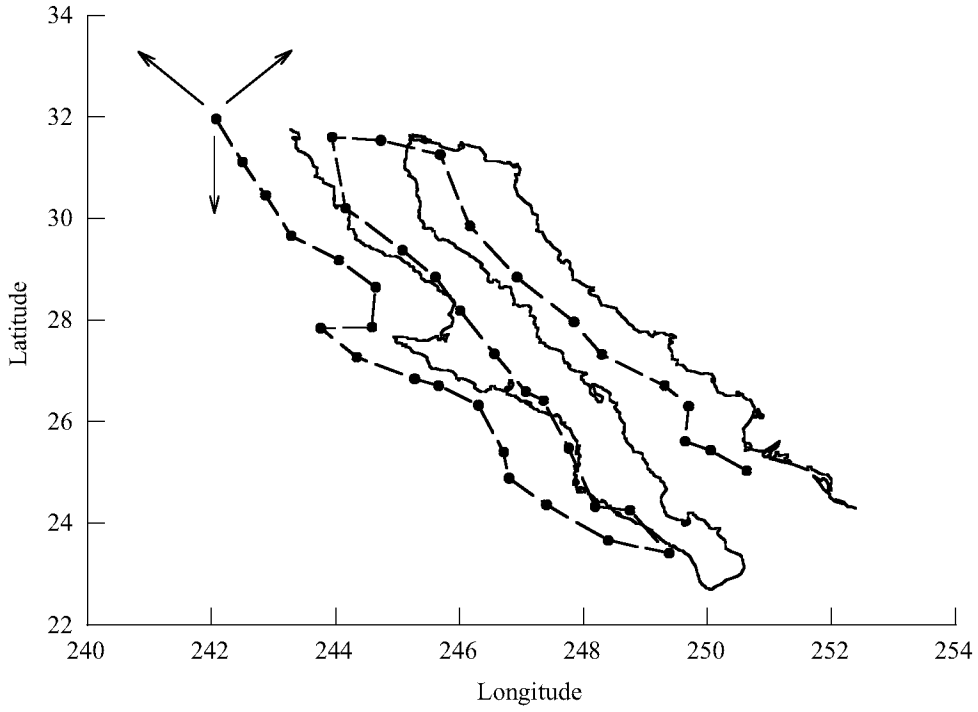

Figure 3. Determination of ensemble geolocation error.

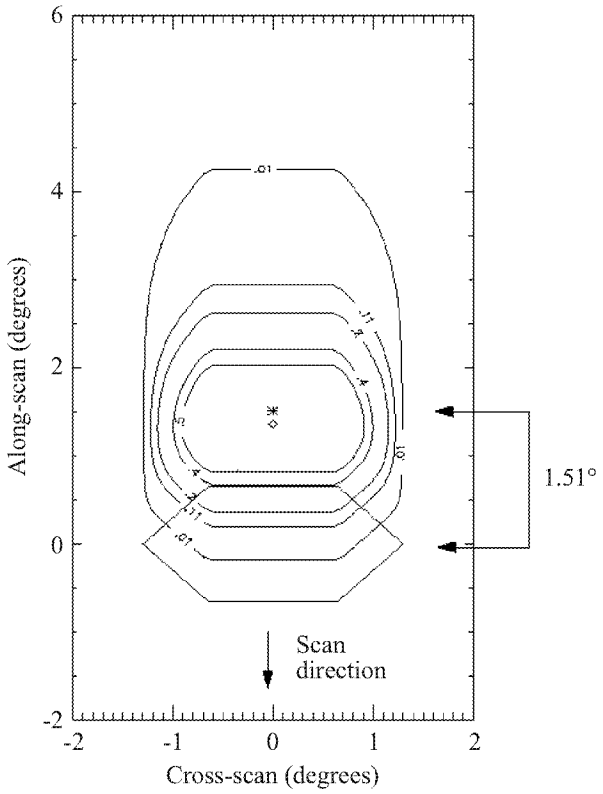

Figure 4. CERES PSF peak and centroid effects on the geolocation process (Smith 1994).

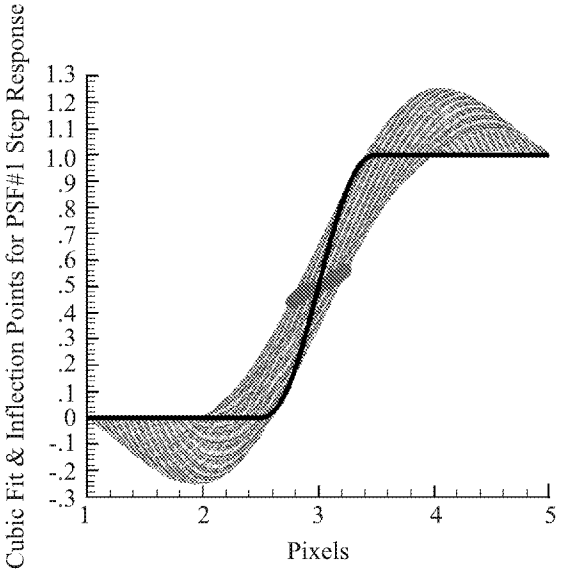

Figure 5. Inflection point uncertainty sampling the CALIPSO PSF step response.

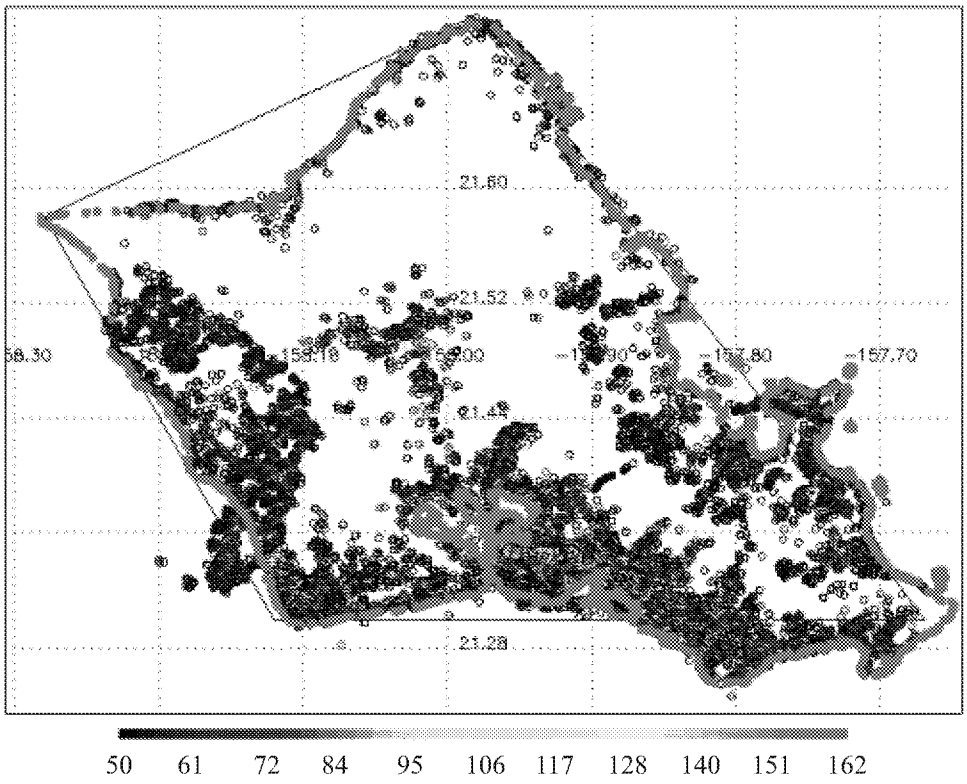

Figure 6. Coastline detections for island of Oahu, Hawaii; ASTER VNIR Band 2, 15 m resolution; June 3, 2000; no cloud filtering; 1:250,000 WVS map (red circles) shifted by detected 900 m bias; color bar indicates radiance in $Wm^{-2}sr^{-1}\mu m^{-1}$).

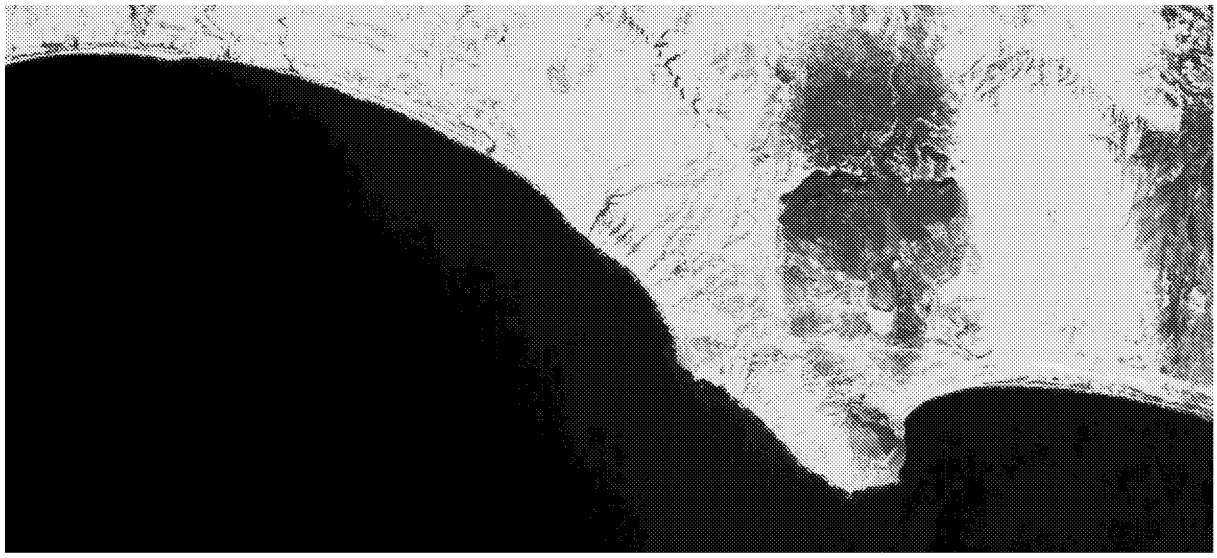

Figure 7. Baja, California; January 29, 2002; ASTER VNIR Band 2, 15 m resolution.

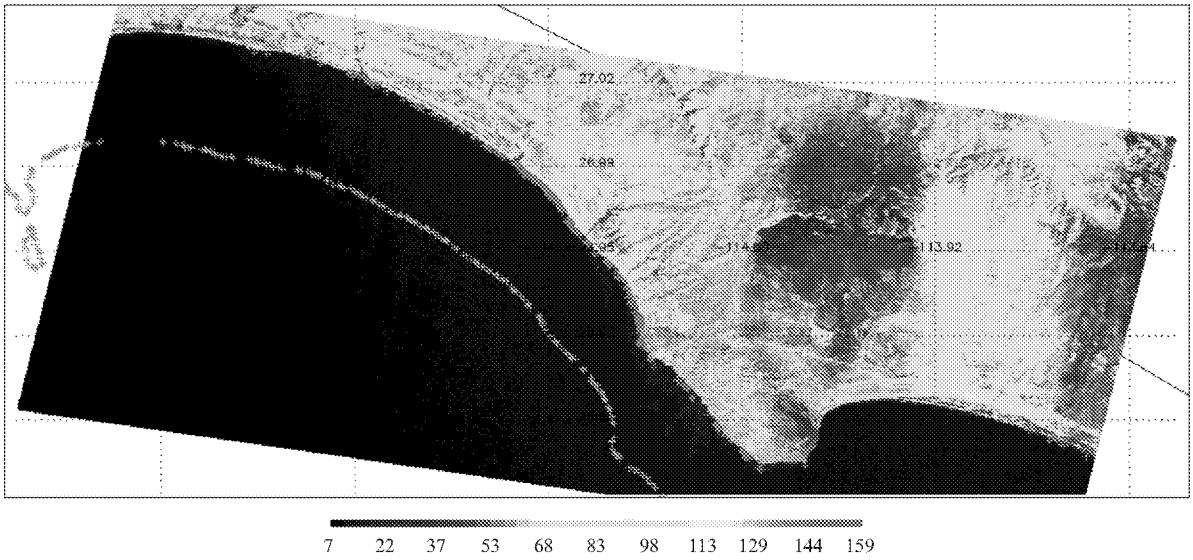

Figure 8. Baja, California; January 29, 2002; coastline crossings detected (red) from ASTER VNIR Band 2, 15 m resolution data; 1:250,000 World Vector Shoreline map (orange) shows geolocation error; color bar indicates radiance in $Wm^{-2}sr^{-1}\mu m^{-1}$.

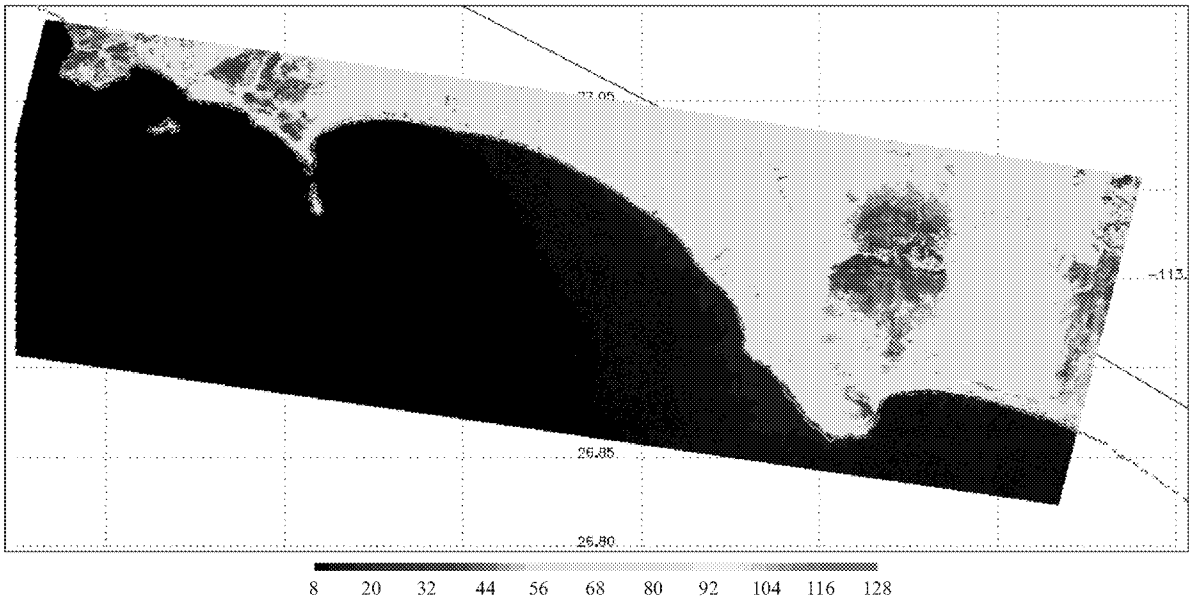

Figure 9. Baja, California; January 29, 2002; World Vector Shoreline map (red) shifted by geolocation error (4.99 km) detected from coastline algorithm; color bar indicates radiance in $Wm^{-2}sr^{-1}\mu m^{-1}$.

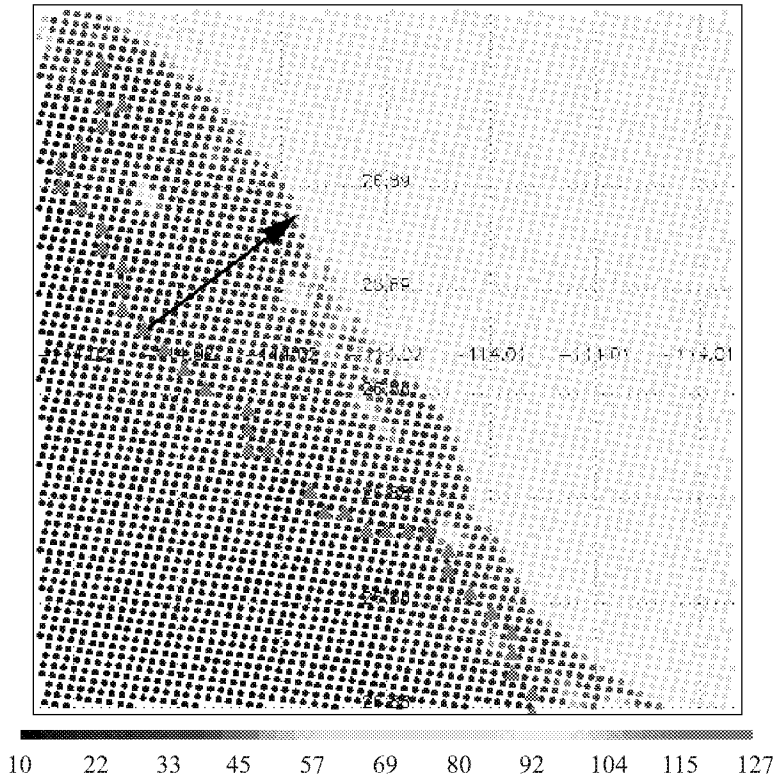

Figure 10. 1:250,000 WVS map points (triangles) 200 m maximum distance from Baja, California coast; January 29, 2002; 15 m ASTER data; color bar indicates radiance in $Wm^{-2}sr^{-1}\mu m^{-1}$.

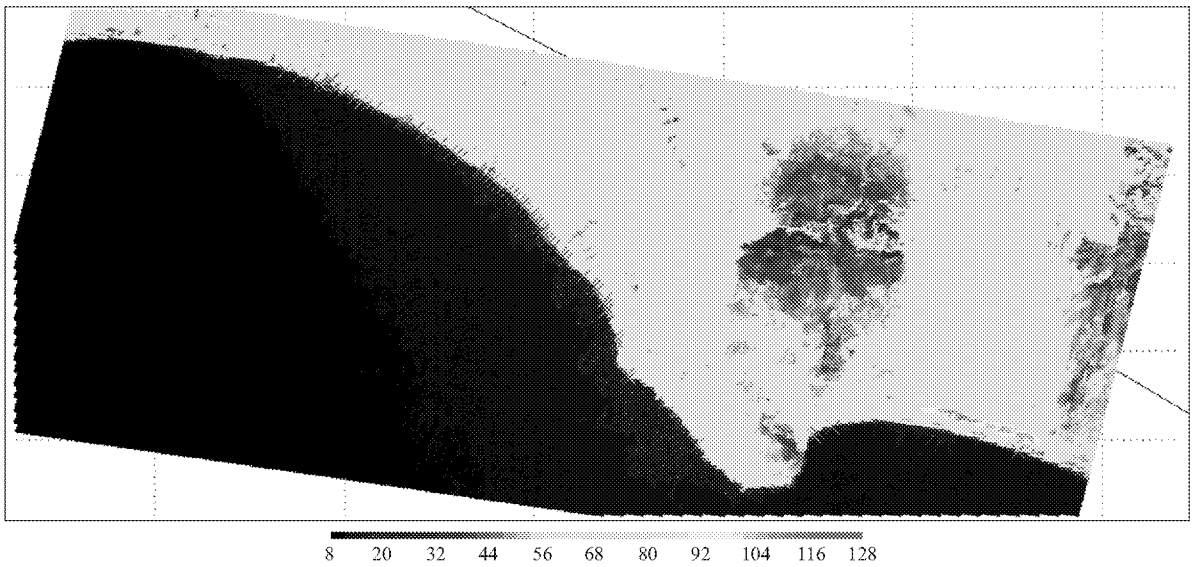

Figure 11. Baja, California; January 29, 2002; coastline crossings (red X's) detected from simulated 125 m resolution WFC data; color bar indicates radiance in $Wm^{-2}sr^{-1}\mu m^{-1}$.

Figure 12. Sarasota Bay, Florida; October 15, 2001; ASTER VNIR Band 2, 15 m resolution.

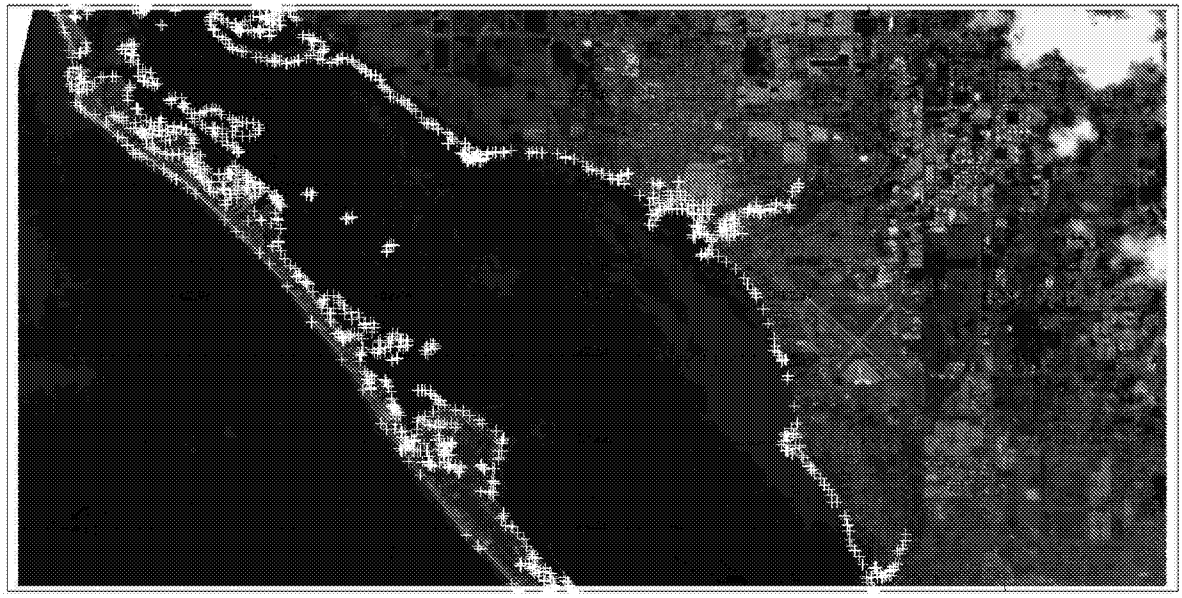

Figure 13. Sarasota Bay, Florida; October 15, 2001; ASTER VNIR Band 2, 15 m resolution; NOAA Medium Resolution Shoreline Map (plus signs) shifted 556 m to match coastline.

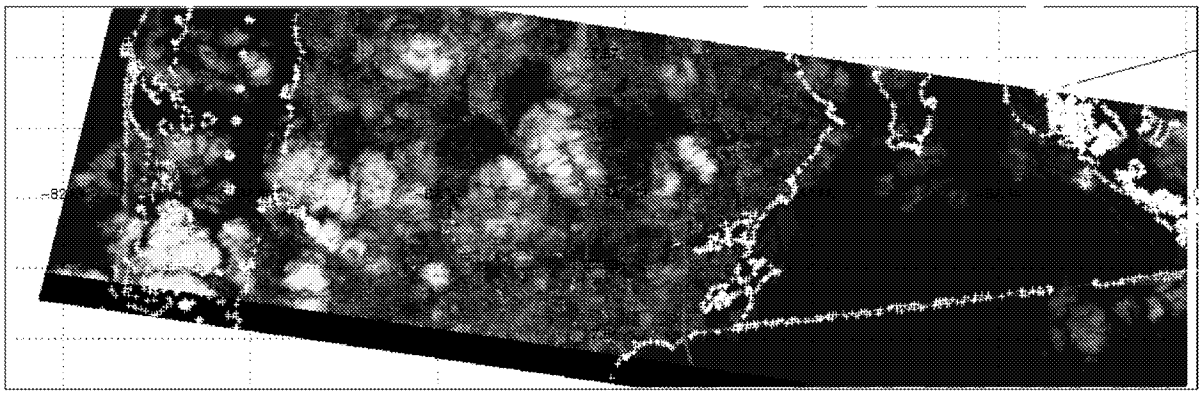

Figure 14. Cloudy scene of Tampa Bay, Florida; October 15, 2001; ASTER VNIR Band 2, 15 m resolution; NOAA Medium Resolution Shoreline Map (plus signs) shifted 1.1 km to match coastline.

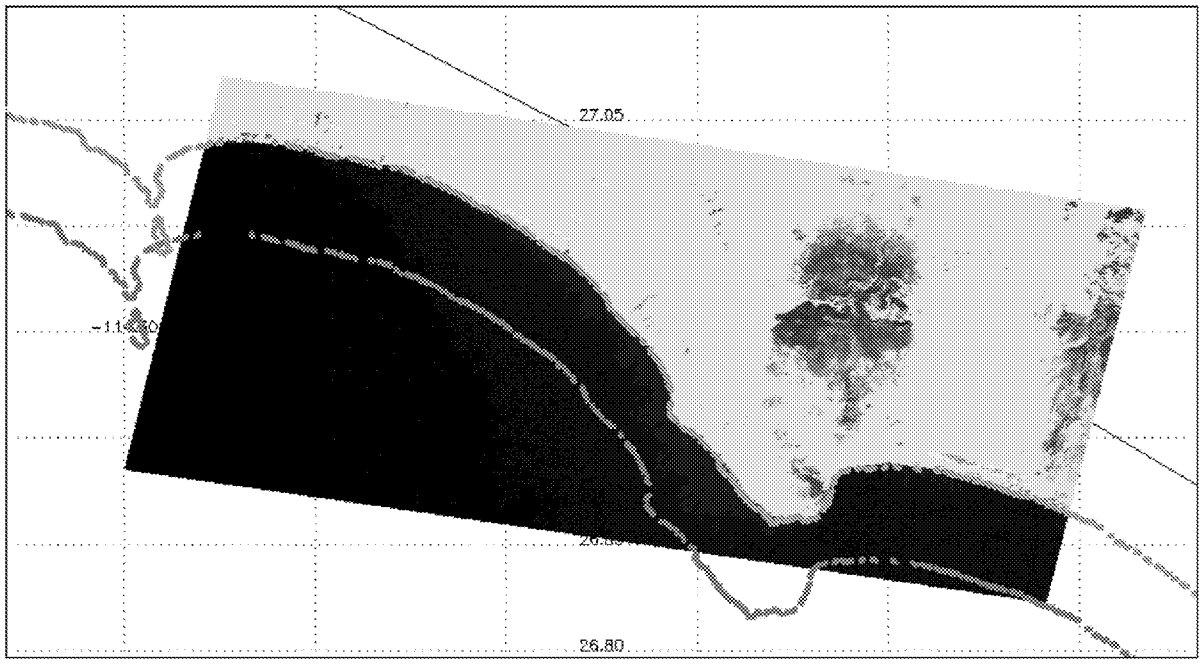

Figure 15. Baja, California; January 29, 2002; interactively shift World Vector Shoreline map (red) to match data coastline (orange); geolocation error calculated interactively agrees to within 41 m of automated coastline results.

Table 1. Instrument footprint resolutions analyzed with the coastline detection algorithm

Instrument	Spacecraft	Nadir Footprint (km)
ERBE	ERBS NOAA-9	40 40
CERES	TRMM Terra Aqua	10 20 20
VIRS	TRMM	2
AIRS	Aqua	13.5

Table 2. Simulated coastline detection inflection point accuracy

PSF Width (pixels)	Shift (pixels)	σ (pixels)	3σ (pixels)
1	0.000	0.176	0.528
2	0.000	0.098	0.294

Table 3. Ensemble map fitting accuracy using crossings extracted from map data

Xings (Factor)	Lon,Lat Shift (degrees)	Start Simplex (degrees)	Detected Lon Shift (degrees)	Detected Lat Shift (degrees)	Total Difference (m)	% Difference	Xing-Map Distance (m)	Number Function Calls
1158 (1/1)	(0, 0)	+/- 1.0	0.00000	0.00000	0.01	N/A	0.02	217
116 (1/10)	(0, 0)	+/- 1.0	0.00000	0.00000	0.01	N/A	0.02	1000
39 (1/30)	(0, 0)	+/- 1.0	0.00000	0.00000	0.02	N/A	0.01	128
1158 (1/1)	(1.2, 0.2)	+/- 2.0	-1.20000	-0.20000	0.34	0.00	0.36	108
116 (1/10)	(1.2, 0.2)	+/- 2.0	-1.20000	-0.20000	0.33	0.00	0.41	112
29 (1/40)	(1.2, 0.2)	+/- 2.0	-1.20000	-0.20000	0.34	0.00	0.27	123
1158 (1/1)	(-0.2, 1.2)	+/- 2.0	0.20000	-1.20000	0.31	0.00	0.37	113
6 (1/200)	(-0.2, 1.2)	+/- 2.0	0.20000	-1.20000	0.36	0.00	0.36	134
4 (1/300)	(-0.2, 1.2)	+/- 2.0	1.07731	-2.74379	197098.09	145.96	10710.00	45
58 (1/20)	(-0.5, -0.5)	+/- 1.0	0.50000	0.50000	0.02	0.00	0.02	112

Table 3. Concluded

Xings (Factor)	Lon,Lat Shift (degrees)	Start Simplex (degrees)	Detected Lon Shift (degrees)	Detected Lat Shift (degrees)	Total Difference (m)	% Difference	Xing-Map Distance (m)	Number Function Calls
58 (1/20)	(0.5, -0.5)	+/- 1.0	-0.50000	0.50000	0.03	0.00	0.02	112
58 (1/20)	(-0.01, -0.01)	+/- 1.0	0.00999	0.01000	0.56	0.04	0.43	101
58 (1/20)	(0.01, -0.01)	+/- 1.0	-0.01000	0.01000	0.55	0.04	0.66	108
1158 (1/1)	(0.001, -0.001)	+/- 2.0	-0.00100	0.00100	0.31	0.20	0.74	93
39 (1/30)	(0.001, -0.001)	+/- 2.0	-0.00101	0.00100	0.65	0.41	0.66	107
1158 (1/1)	(0.0001, 0.0001)	+/- 0.5	-0.00010	-0.00010	0.55	3.50	0.72	93
58 (1/20)	(0.0001, 0.0001)	+/- 0.5	-0.00011	-0.00010	0.74	4.73	0.56	99

Table 4. Coastline algorithm accuracy using ASTER data

Resolution (m)	Xings	Threshold ($w/m^2/sr$)	Lon Shift (degrees)	Lat Shift (degrees)	Mean Shift Detected (m)	σ Shift Detected (m)	Xing-Map (m)
15	543	60	-0.01053	-0.04365	4993	19	95
125	71	50	0.00027	0.00031	48	10	85

REPORT DOCUMENTATION PAGE

Form Approved
OMB No. 0704-0188

1. AGENCY USE ONLY (*Leave blank*)	2. REPORT DATE	3. REPORT TYPE AND DATES COVERED
	November 2002	Technical Publication

4. TITLE AND SUBTITLE
Geolocation Assessment Algorithm for CALIPSO Using Coastline Detection

5. FUNDING NUMBERS
259-40-01-10

6. AUTHOR(S)
J. Chris Currey

7. PERFORMING ORGANIZATION NAME(S) AND ADDRESS(ES)
NASA Langley Research Center
Hampton, VA 23681-2199

8. PERFORMING ORGANIZATION REPORT NUMBER
L-18247

9. SPONSORING/MONITORING AGENCY NAME(S) AND ADDRESS(ES)
National Aeronautics and Space Administration
Washington, DC 20546-0001

10. SPONSORING/MONITORING AGENCY REPORT NUMBER
NASA/TP-2002-211956

11. SUPPLEMENTARY NOTES

12a. DISTRIBUTION/AVAILABILITY STATEMENT
Unclassified-Unlimited
Subject Category 43 Distribution: Standard
Availability: NASA CASI (301) 621-0390

12b. DISTRIBUTION CODE

13. ABSTRACT (*Maximum 200 words*)
Cloud-Aerosol Lidar Infrared Pathfinder Satellite Observations (CALIPSO) is a joint satellite mission between NASA and the French space agency CNES. The investigation will gather long-term, global cloud and aerosol optical and physical properties to improve climate models. The CALIPSO spacecraft is scheduled to launch in 2004 into a 98.2° inclination, 705 km circular orbit approximately 3 minutes behind the Aqua spacecraft. The payload consists of a two-wavelength polarization-sensitive lidar, and two passive imagers operating in the visible (0.645 mm) and infrared (8.7 - 12.0 mm) spectral regions. The imagers are nadir viewing and co-aligned with the lidar. Earth viewing measurements are geolocated to the Earth fixed coordinate system using satellite ephemeris, Earth rotation and geoid, and instrument pointing data. The coastline detection algorithm will assess the accuracy of the CALIPSO geolocation process by analyzing Wide Field Camera (WFC) visible ocean land boundaries. Processing space-time coincident MODIS and WFC scenes with the coastline algorithm will help verify the co-registration requirement with Moderate Resolution Imaging Spectrometer (MODIS) data. This paper quantifies the accuracy of the coastline geolocation assessment algorithm.

14. SUBJECT TERMS	15. NUMBER OF PAGES
Geolocation Assessment; Coastlines; CALIPSO	27
	16. PRICE CODE

17. SECURITY CLASSIFICATION OF REPORT	18. SECURITY CLASSIFICATION OF THIS PAGE	19. SECURITY CLASSIFICATION OF ABSTRACT	20. LIMITATION OF ABSTRACT
Unclassified	Unclassified	Unclassified	UL